



OPEN

# Large magnetoelectric coupling in $\text{Co}_4\text{Nb}_2\text{O}_9$

SUBJECT AREAS:

MAGNETIC PROPERTIES  
AND MATERIALSELECTRONIC PROPERTIES AND  
MATERIALSReceived  
24 October 2013Accepted  
3 January 2014Published  
27 January 2014Correspondence and  
requests for materials  
should be addressed to  
D.H.W. (wangdh@nju.  
edu.cn)Y. Fang<sup>1</sup>, Y. Q. Song<sup>1</sup>, W. P. Zhou<sup>1</sup>, R. Zhao<sup>2</sup>, R. J. Tang<sup>2</sup>, H. Yang<sup>2</sup>, L. Y. Lv<sup>1</sup>, S. G. Yang<sup>1</sup>, D. H. Wang<sup>1</sup> & Y. W. Du<sup>1</sup>

<sup>1</sup>National Laboratory of Solid State Microstructures and Key Laboratory of Nanomaterials for Jiang Su Province, Nanjing University, Nanjing 210093, People's Republic of China, <sup>2</sup>Jiangsu Key Laboratory of Thin Films, School of Physical Science and Technology, Soochow University, Suzhou 215006, China.

Magnetoelectric materials which simultaneously exhibit electric polarization and magnetism have attracted more and more attention due to their novel physical properties and promising applications for next-generation devices. Exploring new materials with outstanding magnetoelectric performance, especially the manipulation of magnetization by electric field, is of great importance. Here, we demonstrate the cross-coupling between magnetic and electric orders in polycrystalline  $\text{Co}_4\text{Nb}_2\text{O}_9$ , in which not only magnetic-field-induced electric polarization but also electric field control of magnetism is observed. These results reveal rich physical phenomenon and potential applications in this compound.

Spin-based electronics combining charge and spin degree of freedom is expected to dominate the next-generation technology that overcomes various difficulties in the conventional charge-based electronic device<sup>1,2</sup>. Acting as an important technique, magnetization manipulated by current has been extensively investigated in metallic and semiconducting materials<sup>3–5</sup>. However, current flow, more or less accompanies energy dissipation, and in this context, insulating materials in which magnetization can be controlled by electric field without major current flow would be fascinating and highly desired. Single-phase magnetoelectric (*ME*) materials are promising candidates for such an operation by fully exploiting their cross-control of magnetism and polarization<sup>6,7</sup>. To attain giant *ME* coupling in such materials, the electric polarization would be preferably induced by magnetic order<sup>7</sup>. Along this line, type-II multiferroics, in which polarization exists only in a magnetically ordered state and is caused by a particular type of magnetic structure, satisfy the requirement well<sup>8</sup>. Since Tokura et al. published the pioneering work on the large *ME* effect in  $\text{TbMnO}_3$ <sup>9</sup>, a great number of type-II multiferroics have been reported these years, such as  $\text{CuO}$ , hexaferrites,  $\text{GdFeO}_3$ ,  $\text{CaMn}_7\text{O}_{12}$ , etc<sup>10–13</sup>. So far as we know, magnetic field control of polarization have been widely exploited in the past decades<sup>9–16</sup>, however, to the contrary, electric manipulation of magnetism is still quite rarely reported<sup>12,17–19</sup>. As mentioned above, electric control of magnetization is expected to play an important role in future technological applications, such as electrical write and magnetic read devices, *ME* random access memories, and so on<sup>20,21</sup>. Therefore, exploration of materials with large *ME* coupling, especially the effect of electric control of magnetism is of primary importance. Besides type-II multiferroics, large coupling between magnetization and electric polarization can be realized in another kind of materials with a different form—the linear *ME* effects. This effect was first investigated in the 1960s and a revival of it is observed recently since large linear *ME* effects have been obtained in many systems, such as  $\text{Cr}_2\text{O}_3$ ,  $\text{MnTiO}_3$ ,  $\text{Ni}_{0.4}\text{Mn}_{0.6}\text{TiO}_3$ ,  $\text{NdCrTiO}_5$ , etc<sup>19,22–26</sup>. Similar to magnetically induced ferroelectricity, this effect occurs in antiferromagnets with broken inversion symmetry as well. At ground state, the electric polarization in these *ME* materials is zero. However, with increasing magnetic field, the polarization would be developed and increase in intensity, showing a linear *ME* effect<sup>27</sup>. Besides these materials,  $\text{Co}_4\text{Nb}_2\text{O}_9$ , which is a collinear antiferromagnet and possesses a magnetic point  $\bar{3}'m'$ <sup>28</sup>, is expected to be a promising candidate as a linear *ME* material from the viewpoint of magnetic symmetry. According to the earlier report by Kolodiazhnyi et al, a dielectric peak is observed in  $\text{Co}_4\text{Nb}_2\text{O}_9$  near the antiferromagnetic phase transition temperature on the condition that an external magnetic field ( $>12$  kOe) is applied. After excluding some possible origin, the authors contribute the giant magnetodielectric effect in  $\text{Co}_4\text{Nb}_2\text{O}_9$  to magnetically-driven spin-flop phase transition. In general, an anomaly in dielectric constant may indicate a sudden change of electric polarization, such as onset or rotation. Therefore, it is very necessary to study the magnetic-field-induced polarization and *ME* effect in this compound. In this manuscript, we prepare a polycrystalline  $\text{Co}_4\text{Nb}_2\text{O}_9$  and investigate its magnetic and electric

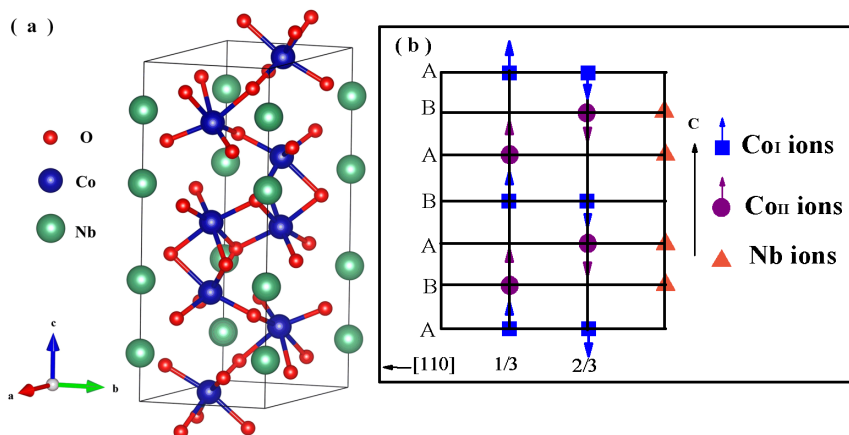


**Figure 1** | (a) The crystalline structure and (b) magnetic structure of  $\text{Co}_4\text{Nb}_2\text{O}_9$ .

properties. Not only the magnetic-induced electric polarization but also an effect of electric field control of magnetization is observed in this *ME* material.

## Results

**Characterization of  $\text{Co}_4\text{Nb}_2\text{O}_9$  polycrystalline sample.**  $\text{Co}_4\text{Nb}_2\text{O}_9$  crystallizes in  $\alpha\text{-Al}_2\text{O}_3$ -type structure (space group  $P\bar{3}C1$ ) with lattice constants of  $a = 5.169(4)$  and  $c = 14.127(9)$  Å<sup>29</sup>, which is schematically illustrated in Fig. 1(a). It is shown that the Co and Nb ions occupy on the Al sites with a ratio of 2:1, where the two crystallographic sites for the Co ions are non-equivalent. The unit cell consists of two formula units built up by three unit cells of the corundum type. The magnetic structure of  $\text{Co}_4\text{Nb}_2\text{O}_9$  has been settled by Bertaut et al. and recently confirmed by Schwarz et al.<sup>28–30</sup> According to the result of neutron diffraction, two non-equivalent octahedral sites are occupied by  $\text{Co}_I$  and  $\text{Co}_{II}$ . The magnetic moments of the Co ions are parallel to  $c$  direction and form chains along the line  $(\frac{1}{3}, \frac{2}{3}, z)$  (spin up) and  $(\frac{2}{3}, \frac{1}{3}, z)$  (spin down), which is plotted in Fig. 1(b), resulting in a collinear antiferromagnetic spin structure with a magnetic point  $\bar{3}'m'$ <sup>30</sup>. This spin configuration is similar to that of  $\text{Cr}_2\text{O}_3$ , which breaks both the space-inversion and time-reversal symmetries and then allows a linear *ME* effect<sup>19</sup>.

Fig. 2 shows X-ray diffraction  $\theta$ - $2\theta$  spectra for the polycrystalline sample at room temperature. It is seen that all the spectra fit the standard database for the single corundum-type structure with space group  $P\bar{3}c1$  well without an impurity phase detected in the apparatus resolution. The temperature dependence of magnetization for  $\text{Co}_4\text{Nb}_2\text{O}_9$  at various external magnetic fields is shown in Fig. 3(a). Under a magnetic field of 0.1 kOe, it is obvious that the magnetization first increases almost linearly with increasing temperature. After reaching a maximum value, the magnetization begins to drop upon warming, showing a typical antiferromagnetic behavior. The peak temperature around 28 K can be defined as the Néel temperature ( $T_N$ ) of  $\text{Co}_4\text{Nb}_2\text{O}_9$ , which is consistent with the earlier report<sup>30</sup>. A similar thermomagnetic curve is observed with magnetic fields of 1 and 10 kOe. However, when the external magnetic field exceeds 20 kOe, the magnetization shows a distinctive behavior: it increases with decreasing temperature and a bump around  $T_N$  is observed, which can be considered as a feature of spin-flop transition of antiferromagnet<sup>31,32</sup>. According to the earlier reports, a large magnetic field applied along the easy axis can lead to the spin-flop transition in  $\text{Co}_4\text{Nb}_2\text{O}_9$ , whereas magnetic field deviating from the easy axis would stabilize the canted spin states. If the external magnetic field is high enough, both spin-flop and canted states would transform into a saturated spin-flip state<sup>30</sup>. Fig. 3(b) plots the variation of

magnetization as a function of external magnetic field for  $\text{Co}_4\text{Nb}_2\text{O}_9$  at 4 K. A change of slope is observed and no sign of saturation is found until the magnetic field reaches up to 60 kOe. As shown in the inset of Fig. 3(b), a field of about 15.7 kOe can be regarded as the critical field to induce the spin flop transition in  $\text{Co}_4\text{Nb}_2\text{O}_9$ , which is evidence by the anomaly in magnetic susceptibilities<sup>31</sup>. Recently, the magnetic induced polarization related to spin-flop phase has been reported in some linear *ME* materials, such as  $\text{Cr}_2\text{O}_3$ ,  $\text{MnTiO}_3$ , etc.<sup>19,23</sup>. Therefore, it is necessary to investigate the electric polarization in the spin-flop phase of  $\text{Co}_4\text{Nb}_2\text{O}_9$ .

**Magnetic field control of electric polarization.** In order to confirm the existence of magnetic induced polarization in  $\text{Co}_4\text{Nb}_2\text{O}_9$ , we carry out the measurement of pyroelectric current, which is collected under various magnetic fields. Before the measurement, *ME* cooling from 70 to 10 K with an electric field of 667 kV/m and a magnetic field of 20, 40 and 70 kOe is applied on the sample. Then the pyroelectric current is recorded with increasing temperature at different external magnetic fields. As shown in Fig. 4, no signal of pyroelectric current is observed at zero magnetic fields. However, in the presence of external magnetic field, the pyroelectric current develops in a temperature interval related to the antiferromagnetic phase transition and the peak values of it increase in intensity with increasing magnetic fields. The inset of Fig. 4 shows the change in sign of pyroelectric current at 70 kOe as a function of temperature with positive and negative poling electric field of 667 kV/m, respectively. A rather symmetric temperature dependence of pyroelectric current curve is observed, indicating that the electric polarization can be reversed by electric

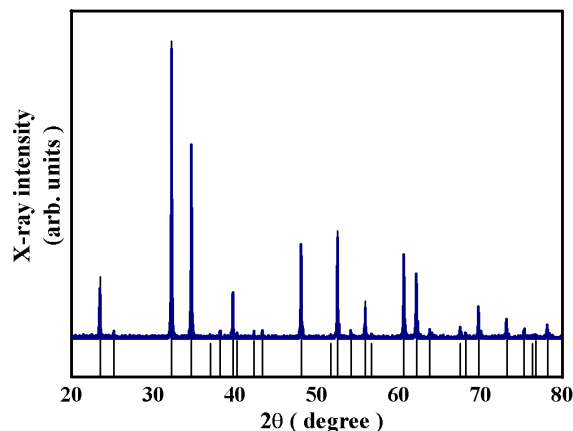


**Figure 2** | XRD pattern of  $\text{Co}_4\text{Nb}_2\text{O}_9$  at room temperature.

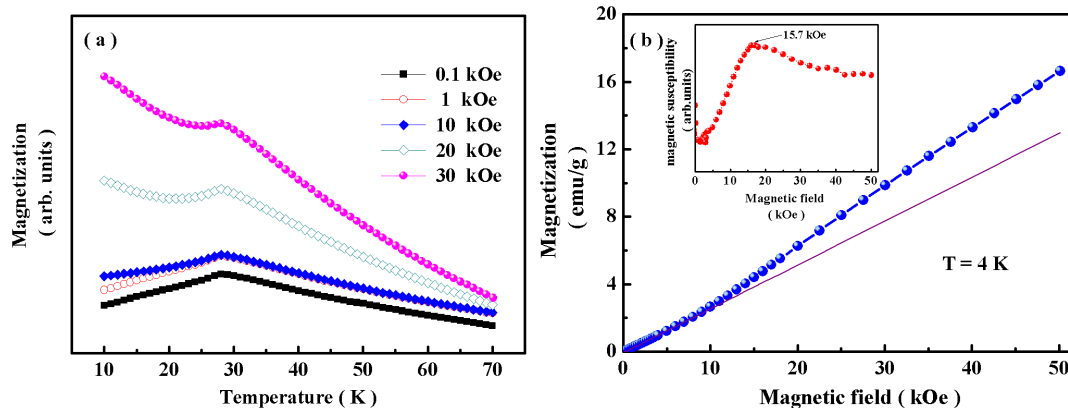


**Figure 3** | (a) The temperature dependence of magnetization under 0.1, 1, 10, 20, 30 kOe, respectively; (b) The magnetization versus magnetic field at 4 K for  $\text{Co}_4\text{Nb}_2\text{O}_9$ ; The inset shows the magnetic susceptibility as a function of magnetic field.

field. This result further shows that the electric polarization behavior is dependent on the *ME* cooling history, which is similar to other linear *ME* material<sup>26</sup>.

The temperature dependence of electric polarization, which is obtained by integration of pyroelectric current with respect to time, is shown in Fig. 5. It is obvious that no spontaneous electric polarization was observed in  $\text{Co}_4\text{Nb}_2\text{O}_9$  without the external magnetic field. However, a magnetic-field-induced polarization of  $30 \mu\text{C}/\text{m}^2$  is observed at 10 K with a field of 20 kOe and the induced polarization increases with the increase of applied magnetic field. As shown in the inset of Fig. 5, polarization increases proportionally with increasing magnetic field, showing a linear *ME* effects. The *ME* susceptibility  $\alpha_{\text{ME}}$  ( $\alpha_{\text{ME}} = \frac{P(H) - P(0)}{\Delta H}$ ) reaches up to  $18.4 \text{ ps}/\text{m}$  at 70 kOe, which is comparable to the reported linear *ME* materials, such as  $\text{MnTiO}_3$  ( $2.6 \text{ ps}/\text{m}$ )<sup>23</sup>,  $\text{NdCrTiO}_5$  ( $0.51 \text{ ps}/\text{m}$ )<sup>26</sup>, indicating a large *ME* coupling in  $\text{Co}_4\text{Nb}_2\text{O}_9$ . It is worth noting that the onset temperature of polarization is consistent with the magnetic ordering temperature of 28 K, suggesting the inherent coupling between the magnetic and electric orders in  $\text{Co}_4\text{Nb}_2\text{O}_9$ .

**Electric field manipulation of magnetization.** For further characterizing the cross-coupling between magnetism and electric polarization, the thermomagnetic curves of  $\text{Co}_4\text{Nb}_2\text{O}_9$  are measured at 0.1 kOe and selected electric fields (0, 1, 2 MV/m). Before the measurement, a *ME* cooling is performed under 40 kOe ( $H \gg H_C$ )

and 1 MV/m in order to ensure the same initial magnetization and electric polarization states of the sample. As shown in Fig. 6(a), the thermomagnetic curves show similar behavior under different electric fields while the magnetization increases remarkably with increasing electric field below 28 K, indicating the manipulation of electric field on magnetization. It is worth noting that the magnetization above  $T_N$  keeps unchanged with applied electric field, which is ascribed to the disappearance of polarization. The change of magnetization at different electric fields is defined as  $\Delta M = M(E) - M(0 \text{ V})$ , which is shown in Fig. 6(b). It is obvious that it increases with decreasing temperature and reaches up to the maximum values of 1.7, 3.3 memu/g at 10 K under 1 and 2 MV/m, respectively. Moreover, Fig. 6(c) shows the time dependence of magnetization under a square wave electric field of 2 MV/m. It is obvious that magnetization decreases or increases with removing or applying electric fields, respectively, indicating a stable response to the electric fields, which further demonstrates the modulation of electric field on magnetization in  $\text{Co}_4\text{Nb}_2\text{O}_9$ .

## Discussion

It is known that  $\text{Co}_4\text{Nb}_2\text{O}_9$  has the same spin configuration as that of  $\text{Cr}_2\text{O}_3$ , which is a time-honored *ME* material<sup>19</sup>. According to the earlier reports about  $\text{Cr}_2\text{O}_3$ , it exhibits spin-flop transition and ferroelectricity provided that a high-enough magnetic field is applied<sup>19,33,34</sup>. The neutron scattering result indicates that, below

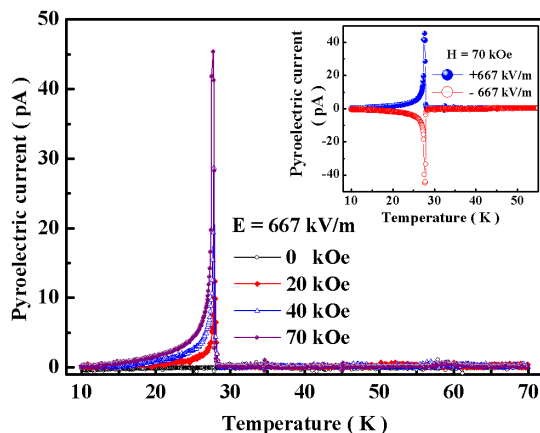


**Figure 4** | The pyroelectric current as a function of temperature under various magnetic fields after *ME* cooling; The inset shows the symmetric current curve under different cooling condition (70 kOe,  $\pm 667 \text{ kV}/\text{m}$ ), respectively.

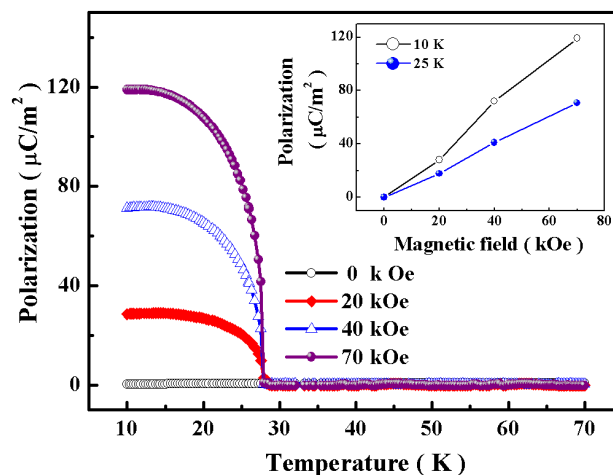


**Figure 5** | (a) The temperature dependence of polarization under various magnetic fields; The inset shows the polarization versus magnetic field at 10 and 25 K, respectively.

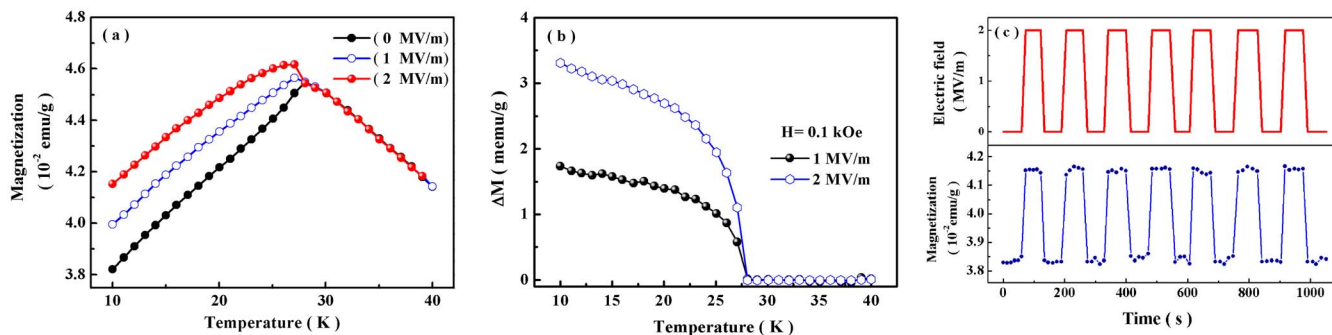


**Figure 6** | (a) The temperature dependence of magnetization under 0, 1 and 2 MV/m after *ME* cooling at 40 kOe, 667 kV/m, respectively; (b) The change of magnetization at different electric fields as a function of temperature; (c) Stable response of magnetization to a periodic electric field as a function of time.

$T_N$ , a staggered magnetization is observed in  $\text{Cr}_2\text{O}_3$  in the presence of external magnetic field. Furthermore, the temperature where staggered magnetization occurs is just the onset temperature of ferroelectricity<sup>35</sup>. Based on these results, Kimura et al. argue that the in-field ferroelectricity in  $\text{Cr}_2\text{O}_3$  would be attributed to this special magnetic order, staggered magnetization<sup>19</sup>. As for  $\text{Co}_4\text{Nb}_2\text{O}_9$ , besides the same crystal and magnetic structures as those of  $\text{Cr}_2\text{O}_3$ , it also shows the spin-flop-induced electric polarization and cross-coupling between polarization and magnetization. Therefore, it is reasonable to ascribe polarization in  $\text{Co}_4\text{Nb}_2\text{O}_9$  to the formation of the magnetic induced spin-flop phase.

Due to the inherent coupling between magnetic and electric orders, changing external magnetic field would modify the spin configuration and the magnitude of polarization, showing the manipulation of magnetic field on polarization. As for the effect of electric field on magnetization, it can be understood as follows: after *ME* cooling, the polarization can be induced below  $T_N$  and an applied electric field would make the net polarization arrange in its direction. Since the magnetism and polarization have the same spin origin, the rearrangement of electric polarization caused by electric field would lead to the rotation of antiferromagnetic regions, and as a consequence, showing the effect of electric field control of magnetization.

In order to understand the linear *ME* effect in  $\text{Co}_4\text{Nb}_2\text{O}_9$ , we can turn to the Ginzburg-Landau expansion of the free energy in terms of electric and magnetic fields ( $\vec{E}$  and  $\vec{H}$ )<sup>26,27</sup>,

$$F(\vec{E}, \vec{H}) = F_0 - P_i^s E_i - M_i^s H_i - \frac{1}{2} \epsilon_0 \epsilon_{ij} E_i E_j - \frac{1}{2} \mu_0 \mu_{ij} H_i H_j - \alpha_{ij} E_i H_j - \dots \quad (1)$$

Where  $\vec{P}^s$  and  $\vec{M}^s$  denote the spontaneous electric polarization and magnetization, whereas,  $\epsilon$  and  $\mu$  are the electric and magnetic susceptibilities. Differentiation with respect to the electric fields leads to electric polarization,

$$P_i(\vec{E}, \vec{H}) = - \frac{\partial F}{\partial E_i} = P_i^s + \epsilon_0 \epsilon_{ij} E_j + \alpha_{ij} H_j + \dots \quad (2)$$

The tensor  $\alpha$  corresponds to the induction of electric polarization by a magnetic field<sup>26,27</sup>. In the case of  $\text{Co}_4\text{Nb}_2\text{O}_9$ , the spontaneous electric polarization is zero at ground state and a magnetic field can induce a finite electric polarization, which increases with increasing field, indicating a linear *ME* effect.

In conclusion, we have performed detail measurements on *ME* properties of polycrystalline  $\text{Co}_4\text{Nb}_2\text{O}_9$ . The experimental results reveal that no spontaneous polarization arises below  $T_N$  unless a high enough magnetic field is applied. The polarization increases proportionally with the applied magnetic field, showing a linear *ME* effects. Different from most reported *ME* materials, an effect of electric

control magnetization is observed in this compound. The attractive cross-control between electric polarization and magnetism in  $\text{Co}_4\text{Nb}_2\text{O}_9$  demonstrates an avenue for next generation and low-energy consumption spintronics.

## Methods

**Sample preparation.** Polycrystalline sample of  $\text{Co}_4\text{Nb}_2\text{O}_9$  was prepared by solid state reaction method. The stoichiometric mixtures of pure  $\text{Co}_3\text{O}_4$  and  $\text{Nb}_2\text{O}_5$  were well ground and annealed at 1173 K for 10 h in muffle furnace. The resulting powders were then pressed into pellets with a 12 mm diameter under 40 MPa. Finally, the pellets were sintered in air at 1373 K for 5 h followed by cooling down to room temperature. The structure of as-prepared sample was checked using X-ray diffraction (XRD, Bruker Corporation) equipped with  $\text{Cu K}\alpha$  radiation at room temperature. The resistivity of  $\text{Co}_4\text{Nb}_2\text{O}_9$  at room temperature exceeds  $6 \times 10^9 \Omega\text{-cm}$ , which is high enough to support an electric field and ensures the *ME* measurements.

**Magnetic and electric measurements.** Magnetic properties were measured by superconducting quantum interference device (SQUID, Quantum Design) magnetometer with applied magnetic fields of 0.1, 1, 10, 20, 30 kOe, respectively. As-prepared sample was polished into a thin disk of 0.3 mm in thickness and Au electrodes were sputtered on both sides for electric measurements, which were carried out by Physical Property Measurement System (PPMS, Quantum Design). Pyroelectric current was collected using an electrometer (Keithley 6514A) after poling the sample in an electric field. In detail, the sample was first submitted to the PPMS and cooled down to 70 K. Then a poling electric field of 667 kV/m was applied on the sample with temperature decreasing from 70 to 10 K. In order to release any charges accumulated on the sample surfaces or inside the sample, the sample was short-circuited for long-enough time. During the recording of pyroelectric current, the sample was heated slowly at a warming rate of 3 K/min. Noted that the magnetic field was applied throughout the cooling and warming processes. After *ME* cooling (1 MV/m, 40 kOe) the sample from 40 to 10 K, the temperature dependence of magnetization was measured under 0.1 kOe with selected electric fields (0, 1, and 2 MV/m). For further investigating the response of magnetization to electric field, the variation of magnetization as a function of a periodic electric field was also measured.

1. Wolf, S. A. *et al.* Spintronics: A spin-based electronics vision for the future. *Science* **294**, 1488–1495 (2001).
2. Žutić, I., Fabian, J. & Das Sarma, S. Spintronics: fundamentals and applications. *Rev. Mod. Phys.* **76**, 323–410 (2004).
3. Mangin, S. *et al.* Current-induced magnetization reversal in nanopillars with perpendicular anisotropy. *Nature Mater.* **5**, 210–215 (2006).
4. Özyilmaz, B. *et al.* Current-induced magnetization reversal in high magnetic fields in Co/Cu/Co nanopillars. *Phys. Rev. Lett.* **91**, 067203 (2003).
5. Chiba, D., Sato, Y., Kita, T., Matsukura, F. & Ohno, H. Current-driven magnetization reversal in a ferromagnetic semiconductor (Ga,Mn)As/GaAs/(Ga,Mn)As tunnel junction. *Phys. Rev. Lett.* **93**, 216602 (2004).
6. Eerenstein, W., Mathur, N. D. & Scott, J. F. Multiferroic and magnetoelectric materials. *Nature* **442**, 759–765 (2006).
7. Cheong, S.-W. & Mostovoy, M. Multiferroics: A magnetic twist for ferroelectricity. *Nature Mater.* **6**, 13–20 (2007).
8. Tokura, Y. Multiferroics-toward strong coupling between magnetization and polarization in a solid. *J. Magn. Magn. Mater.* **310**, 1145–1150 (2007).
9. Kimura, T. *et al.* Magnetic control of ferroelectric polarization. *Nature* **426**, 55–58 (2003).
10. Kimura, T., Sekio, Y., Nakamura, H., Siegrist, T. & Ramirez, A. P. Cupric oxide as an induced-multiferroic with high- $T_c$ . *Nature Mater.* **7**, 291–294 (2008).



11. Ishiwata, S., Taguchi, Y., Murakawa, H., Onose, Y. & Tokura, Y. Low magnetic-field control of electric polarization vector in a helimagnet. *Science* **319**, 1643–1646 (2008).
12. Tokunaga, Y. *et al.* Composite domain walls in a multiferroic perovskite ferrite. *Nature Mater.* **8**, 558–562 (2009).
13. Johnson, R. D. *et al.* Giant Improper Ferroelectricity in the Ferroaxial Magnet  $\text{CaMn}_7\text{O}_{12}$ . *Phys. Rev. Lett.* **108**, 067201 (2012).
14. Choi, Y. J. *et al.* Thermally or Magnetically Induced Polarization Reversal in the Multiferroic  $\text{CoCr}_2\text{O}_4$ . *Phys. Rev. Lett.* **102**, 067601 (2009).
15. Taniguchi, K., Abe, N., Ohtani, S. & Arima, T. Magnetolectric Memory Effect of the Nonpolar Phase with Collinear Spin structure in multiferroic  $\text{MnWO}_4$ . *Phys. Rev. Lett.* **102**, 147201 (2009).
16. Kitagawa, Y. *et al.* Low-field magnetolectric effect at room temperature. *Nature Mater.* **9**, 797–802 (2010).
17. Choi, Y. J., Zhang, C. L., Lee, N. & Cheong, S.-W. Cross-Control of Magnetization and Polarization by Electric and Magnetic fields with competing multiferroic and weak-ferromagnetism phase. *Phys. Rev. Lett.* **105**, 097201 (2010).
18. Chun, S. H. *et al.* Electric Field Control of Nonvolatile Four-State Magnetization at Room temperature. *Phys. Rev. Lett.* **108**, 177201 (2012).
19. Iyama, A. & Kimura, T. Magnetolectric hysteresis loops in  $\text{Cr}_2\text{O}_3$  at room temperature. *Phys. Rev. B* **87**, 180408(R) (2013).
20. Scott, J. F. Applications of modern ferroelectrics. *Science* **315**, 954–959 (2007).
21. Bibes, M. & Barthélémy, A. Multiferroics: Towards a magnetolectric memory. *Nature Mater.* **7**, 425–426 (2008).
22. Freeman, A. J. & Schmid, H. (eds) Magnetolectric Interaction Phenomena in Crystals (Gordon and Breach, London, 1975).
23. Mufti, N. *et al.* Magnetolectric coupling in  $\text{MnTiO}_3$ . *Phys. Rev. B* **83**, 104416 (2011).
24. Yamaguchi, Y. & Kimura, T. Magnetolectric control of frozen state in a toroidal glass. *Nat. Commun.* **4**, 2063 (2013).
25. Yamaguchi, Y., Nakano, T., Nozue, Y. & Kimura, T. Magnetolectric Effect in an XY-like Spin Glass System  $\text{Ni}_x\text{Mn}_{1-x}\text{TiO}_3$ . *Phys. Rev. Lett.* **108**, 057203 (2012).
26. Hwang, J., Choi, E. S., Zhou, H. D., Lu, J. & Schlottmann, P. Magnetolectric effect in  $\text{NdCrTiO}_5$ . *Phys. Rev. B* **85**, 024415 (2012).
27. Fiebig, M. Revival of the magnetolectric effect. *J. Phys. D* **38**, R123–R152 (2005).
28. Bertaut, E. F., Corliss, L., Forrat, F., Aleonard, R. & Pauthenet, R. Etude de niobates et tantalates de métaux de transition bivalents. *J. Phys. Chem. Solids* **21**, 234 (1961).
29. Schwarz, B., Kraft, D., Theissmann, R. & Ehrenberg, H. Magnetic properties of the  $(\text{Co}_x\text{Mn}_{1-x})_4\text{Nb}_2\text{O}_9$  solid solution series. *J. Magn. Magn. Mater.* **322**, L1 (2010).
30. Kolodiazhnyi, T., Sakurai, H. & Vittayakorn, N. Spin-flop driven magneto-dielectric effect in  $\text{Co}_4\text{Nb}_2\text{O}_9$ . *Appl. Phys. Lett.* **99**, 132906 (2011).
31. Hwang, J. *et al.* Magnetic transitions and magnetodielectric effect in antiferromagnet  $\text{SrNdFeO}_4$ . *Phys. Rev. B* **85**, 224429 (2012).
32. Wang, X. Y., Wang, L., Wang, Z. M., Su, G. & Gao, S. Coexistence of Spin-Canting, Metamagnetism, and Spin-Flop in a (4, 4) Layered Manganese Azide Polymer. *Chem. Mater.* **17**, 6369–6380 (2005).
33. Belov, D. V., Vorob'ev, G. P., Kadomtseva, A. M. & Popov, Y. F. Magnetolectric effect in the spin-flop phase of  $\text{Cr}_2\text{O}_3$  and the problem of determining the magnetic structure. *JETP Lett.* **58**, 579 (1993).
34. Fiebig, M., Fröhlich, D. & Thiele, H.-J. Determination of spin direction in the spin-flop phase of  $\text{Cr}_2\text{O}_3$ . *Phys. Rev. B* **54**, R12681–R12684 (1996).
35. Samuelsen, E. J., Hutchings, M. T. & Shirane, G. Inelastic neutron scattering investigation of spin waves and magnetic interactions in  $\text{Cr}_2\text{O}_3$ . *Physica* **48**, 13 (1970).

## Acknowledgments

This work is supported by the National Basic Research Program of China (2012CB932304 and 2009CB929501), National Natural Science Foundation of China (Grant No. 11174130, U1232110, K110813412, 11004145, 11274237, and 51228201), and the Natural Science Foundation of Jiangsu Province under Grant No. SBK201021263.

## Author contributions

Experiments were designed by Y.F. and D.H.W. and carried out by Y.F., W.P.Z., R.Z., R.J.T., H.Y. and L.Y.L. The data were collected by Y.F. Results were analyzed and interpreted by Y.F., Y.Q.S., S.G.Y., D.H.W., Q.Q.C. and Y.W.D. The manuscript was written by Y.F. and D.H.W. D.H.W. and Y.F. are responsible for project direction, planning and infrastructure.

## Additional information

**Competing financial interests:** The authors declare no competing financial interests.

**How to cite this article:** Fang, Y. *et al.* Large magnetolectric coupling in  $\text{Co}_4\text{Nb}_2\text{O}_9$ . *Sci. Rep.* **4**, 3860; DOI:10.1038/srep03860 (2014).



This work is licensed under a Creative Commons Attribution-NonCommercial-NoDerivs 3.0 Unported license. To view a copy of this license, visit <http://creativecommons.org/licenses/by-nc-nd/3.0>